Plasma membrane calcineurin B-like calcium-ion sensor proteins function in regulating primary root growth and nitrate uptake by affecting global phosphorylation patterns and microdomain protein distribution

Liang-Cui Chu, Jan Niklas Offenborn, Leonie Steinhorst, Xu Na Wu, Lin Xi, Zhi Li, Aurore Jacquot, Laurence Lejay, Jörg Kudla

MS LEONIE STEINHORST (Orcid ID : 0000-0002-1592-2732)

DR XU NA WU (Orcid ID : 0000-0002-1288-1349)

DR LAURENCE LEJAY (Orcid ID : 0000-0003-0785-3893)

PROF. JÖRG KUDLA (Orcid ID : 0000-0002-8238-767X)

DR WALTRAUD X SCHULZE (Orcid ID : 0000-0001-9957-7245)

Article type : - Regular Manuscript

Plasma membrane CBL Ca^{2+} sensor proteins function in regulating primary root growth and nitrate uptake by affecting global phosphorylation patterns and microdomain protein distribution

Liang-Cui Chu [1], Jan Niklas Offenborn [2], Leonie Steinhorst [2], Xu Na Wu [1], Lin Xi [1], Zhi Li [1], Aurore Jacquot [3], Laurence Lejay [3], Jörg Kudla [2], Waltraud X. Schulze [1]

[1] Department of Plant Systems Biology, University of Hohenheim, 70593 Stuttgart, Germany

[2] Institut für Biologie und Biotechnologie der Pflanzen, Westfälische Wilhelms-Universität Münster, Schlossplatz 7, 48149 Münster, Germany

[3] BPMP, Univ Montpellier, CNRS, INRAE, Institut Agro, 34060 Montpellier, France

Address for correspondence

Department of Plant Systems Biology

University of Hohenheim (190d)

70593 Stuttgart
Germany
wschulze@uni-hohenheim.de

Received: 11 August 2020
Accepted: 27 September 2020

Summary

- The collective function of Calcineurin B-like (CBL) Ca^{2+} sensors and CBL interacting protein kinases (CIPKs) in decoding plasma membrane initiated Ca^{2+} signals to convey developmental and adaptive responses to fluctuating nitrate availability remained to be determined.
- Here, we generated a *cbl*-quintuple mutant in *Arabidopsis thaliana* devoid of these Ca^{2+} sensors at the plasma membrane and performed comparative phenotyping, nitrate flux determination, phosphoproteome analyses and studies of membrane domain protein distribution in response to low and high nitrate availability.
- We observed that CBL proteins exert multifaceted regulation of primary and lateral root growth and nitrate fluxes. Accordingly, we found that loss of plasma membrane Ca^{2+} sensor function simultaneously affected protein phosphorylation of numerous membrane proteins including several nitrate transporters, proton pumps and aquaporins as well as their distribution within plasma membrane microdomains and identified specific phosphorylation and domain distribution pattern during distinct phases of low and high of nitrate responses.
- Collectively, these analyses reveal a central and coordinative function of CBL-CIPK mediated signalling in conveying plant adaptation to fluctuating nitrate availability and identify a crucial role of Ca^{2+} signalling in regulating the composition and dynamics of plasma membrane microdomains.

Keywords

CIPK/CBL, Ca^{2+} signaling, plasma membrane, protein phosphorylation, membrane microdomain, nitrate signaling, *Arabidopsis thaliana*

Introduction

The plasma membrane separates the cellular interior from its environment, provides an interface for information exchange and processing, and serves as regulative barrier for ion and metabolite exchange. Accordingly, receptor and signaling components as well as transport proteins constitute a significant fraction of plasma membrane localized proteins. Increasing evidence supports the importance of lateral segregation and dynamic membrane subdomain assembly as regulatory means in these processes. In this way signaling complexes can exert their regulatory impact on membrane transport proteins for many nutrients including nitrate.

Nitrate represents a major nitrogen source and important macronutrient for plants (Crawford, 1995; Wang *et al.*, 2012; Vidal *et al.*, 2020). Soil nitrate availability profoundly influences plant growth and architecture, and consequently crop yield (Krouk *et al.*, 2010; Krapp *et al.*, 2014). Nitrate uptake from soil is facilitated by members of the NRT/NPF protein family (Leran *et al.*, 2014). Distinct members of this protein family constitute two complementary systems for nitrate uptake into plants: The low affinity transport system (LATS) and the high affinity transport system (HATS) (Wang *et al.*, 2012). The LATS works with nitrate affinities in millimolar ranges, while HATS exhibits affinities in micromolar ranges. Ammonium serves as alternative nitrogen source for plants and reciprocal interactions between nitrate and ammonium uptake processes were reported (Gazzarrini *et al.*, 1999; Camanes *et al.*, 2012). Nitrate and ammonium availability impact on cellular signaling and regulatory networks by modulating protein modifications and abundance, as well as gene expression (Scheible *et al.*, 2004; Engelsberger & Schulze, 2012; Menz *et al.*, 2016).

Soil nitrate availability also impacts on plant morphology with distinct consequences for primary and lateral roots. In general, nitrogen limitation causes allocation of resources to promote root-system expansion for nutrient foraging resulting in an increased root-to-shoot ratio (Hermans *et al.*, 2006). While growth of primary roots positively correlates with increasing nitrate concentration, regulation of lateral root growth is more complex (Mlodzinska *et al.*, 2015). Low nitrate conditions (LN) stimulate lateral root growth, but high nitrate concentrations (HN) impede lateral root initiation and elongation (Remans *et al.*, 2006). As consequence, under nitrate limiting conditions, expanding lateral root system can explore a larger soil area for available resources. These morphological adaptations are accompanied by dramatic adjustments of ion transport systems.

The nitrate transport system of plants is embedded in complex regulatory networks of mutual interactions, which also involve plasma membrane (PM) localized proton pumps that contribute to energization of nitrate transport and aquaporins that affect cellular water status (Wu *et al.*, 2013; Fuglsang *et al.*, 2014; Haruta *et al.*, 2014). Primary signaling of nitrate availability has been reported to involve cytoplasmic Ca^{2+} signals (Riveras *et al.*, 2015). Accordingly, Ca^{2+} sensors CBL1 and CBL9 in combination with their interacting kinase CIPK23 bring about regulation of the nitrate transceptor NPF6.3/NRT1.1 which plays also a central role in the nitrate dependent regulation of root development (Remans *et al.*, 2006; Ho *et al.*, 2009; Krouk *et al.*, 2010). Phosphorylation status of NPF6.3/NRT1.1 also modulates the nitrate dependent expression induction of NRT2.1 which represents a major facilitator of nitrate uptake. Another family of Ca^{2+}-dependent kinases, the CDPKs (in Arabidopsis designated as CPKs) interconnect these primary signaling events with the regulation of nitrate responsive transcription factors (Liu *et al.*, 2017; Liu *et al.*, 2020).

CBL-type Ca^{2+} sensors and their interacting CIPKs fulfil multifaceted roles in nitrate signaling and regulation of nitrate transport. Kinase CIPK23 was not only shown to regulate the nitrate transceptor NPF6.3/NRT1.1 (Ho *et al.*, 2009), but also inhibits ammonium uptake by C-terminal phosphorylation of ammonium transporters (Straub *et al.*, 2017), and activates potassium channel AKT1 (Sanchez-Barrena *et al.*, 2020). Moreover, related kinase CIPK8 positively regulates primary nitrate response including the induction of NPF6.3/NRT1.1, but negatively regulates long-term nitrate-mediated root growth (Hu *et al.*, 2009). In general, CBLs and CIPKs form a versatile signaling network that in Arabidopsis consists of 10 Ca^{2+} sensors and 26 CIPKs (Kolukisaoglu *et al.*, 2004; Weinl & Kudla, 2009). Various CBL-CIPK complexes were implicated in regulating ion fluxes and ROS production at the PM but also ATPase activity and ion transport at the tonoplast (Xu *et al.*, 2006; Tang *et al.*, 2012; Eckert *et al.*, 2014; Han *et al.*, 2019). While tonoplast targeting of CBLs is brought about by S-acylation, dual lipid modification by myristoylation and S-acylation confers plasma membrane attachment of these Ca^{2+} sensors and their interacting kinases (Batistic *et al.*, 2008; Batistic *et al.*, 2012). Of the ten CBL proteins in Arabidopsis, five, namely CBL1, CBL4, CBL5, CBL8 and CBL9, were found to localize at the PM and thereby to constitute the Ca^{2+} sensing/decoding module of the CBL-CIPK network at this compartment.

The S-acylation status of proteins was shown to affect their subcellular sorting and assembly into plasma membrane subdomains (Rocks *et al.*, 2005; Sorek *et al.*, 2007). Increasing evidence supports the importance of dynamic assembly and regulation of such membrane domains for plant signaling processes. Initially, a biochemical representation of such membrane microdomains became accessible through preparation of detergent resistant membrane (DRM) fractions (Zauber *et al.*, 2013). More recently, modern microscopic

approaches have further aided the understanding of motility of domain associated proteins (Bhat & Panstruga, 2005; Malinsky *et al.*, 2013). Thereby, the stimulus-triggered dynamics of domain assembly and protein motility was investigated for NADPH oxidases, aquaporins and in the context of ABA regulated anion channels (Demir *et al.*, 2013; Hao *et al.*, 2014; Martiniere *et al.*, 2019). In the latter case ABA signaling modulated nanodomain association of the S-acylated Ca^{2+}-dependent kinase CPK21 and thereby affected its ability to phosphorylate ion channel SLAH3 (Demir *et al.*, 2013; Saito *et al.*, 2018).

Despite well-established importance of lipid modification for CBL Ca^{2+} sensor function, their interrelation with plasma membrane domain dynamics and regulation in plants is much less appreciated. Moreover, network-like characteristics of the CBL-CIPK signaling system which confer robustness against perturbations by loss-of-function of single components of this network has hampered the full appreciation of the role of this network for decoding Ca^{2+} signals emanating at the plasma membrane. This holds especially true for the role of CBLs and CIPKs in signal- and response-reactions triggered by fluctuating nitrate availability.

Here we report the generation of a quintuple *cbl1/4/5/8/9* mutant that is devoid of all CBL Ca^{2+} sensors at the plasma membrane. We use this resource to characterize the collective importance of CBL-conferred plasma membrane Ca^{2+} signaling in regulating morphological and molecular nitrate responsiveness. Moreover, we characterize the impact of impaired whole PM Ca^{2+} signaling on the plant phosphoproteome in response to altered nitrate supply and identify several ion flux conducting proteins as clients of this regulation. Finally, we uncover a modulating impact of PM born Ca^{2+} signaling on the composition and dynamics of membrane microdomains.

Materials and Methods

Plant material – Arabidopsis wild type (Col-0) seeds were propagated in the greenhouse at University of Hohenheim, Stuttgart, Germany. The quintuple mutant *cbl 1/4/5/8/9* (*cbl1- 1*, At4g17615 (*WS*), NASC N9888; *cbl4- 2*, At5g24270, GK-015F02; *cbl5-2,* At4g01420, GK-278H02; *cbl8- 1*, At1g64480, SALK_083553; *cbl9- 1*, At5g47100, SAIL-1173-A9) was generated as described. Genotyping was performed by PCR and specific primer sets (Supplementary Table S1).

Hydroponic culture – Surface sterilized seeds were transferred to the hydroponic culture system (Schlesier *et al.*, 2003) for cultivation on the shaker in the growth chamber (16/8h day/night, 22 °C, and 110 ± 10 μEs^{-1} m^{-2}). Details on the growth medium are given in the Supplementary Methods.

Plate assay for root phenotype – Surface sterilized seeds after two days vernalization were first plate on ½ MS medium with 0.5% sucrose for 3 days germination. Seedlings with same growth status were then selected and transferred to different treatment plates for vertical growth. The same medium was used as for hydroponic culture and added 8.0 g/l agar (Duchefa Biochemie). Plates were scanned every two days (Epson Perfection V370) and roots were measured and analyzed by EZ-R_{HIZO} (Armengaud *et al.*, 2009).

Microsomal fraction isolation – The method was adapted from a previous publication (Pertl *et al.*, 2001) as detailed in Supplementary Methods.

Detergent treatment and detergent resistant membrane isolation – Since in our experiment only 1 g of root material was used, it was important to keep protein loss at a minimum, and therefore, detergent treatment was directly performed on microsomal fractions. MF equivalent to 500 µg protein was used for each sample and mixed with detergent Triton X-100 and TNE buffer (25 mM Tris-HCl, pH 7.5, 150 mM NaCl and 5 mM EDTA) to reach the final concentration of 2% detergent and the detergent to protein ratio of 10:1 (w/w). The mixture was incubated at 4 °C during detergent treatment. Sample were then adjusted final concentration of 1.8 M sucrose and transferred to the bottom of ultracentrifuge tube. Then, 4 mL of 1.6 M, 3.5 mL of 1.4 M and 1.5 mL of 0.15 M sucrose (in TNE buffer) were sequentially layered on top of detergent-treated MF to form a sucrose step gradient as published previously (Szymanski *et al.*, 2013).

Detergent removal, tryptic digestion and peptide desalting – Instead of precipitating protein from the detergent containing samples we used filter-aided sample preparation (Wisniewski *et al.*, 2009) method to remove detergent from samples and meanwhile reduce protein loss. All the steps were processed at room temperature (24° C) as described in Supplementary Methods.

Phosphopeptides enrichment – Phosphopeptides were studied in parallel with microdomain distribution samples and were enriched via TiO_2 beads as described (Wu *et al.*, 2017) as detailed in Supplementary Methods.

LC-MS/MS analysis of peptides and phosphopeptides – Peptides mixtures were analyzed by HPLC system nanoflow Easy-nLC (Thermo Scientific) and Orbitrap hybrid mass spectrometer (Q-exactive, Thermo Scientific) as described previously (Wu *et al.*, 2019) and detailed in Supplementary Methods.

Protein identification and label free quantification of protein intensities – MaxQuant version 1.5.3.8 (Cox & Mann, 2008) was used for raw file peak extraction and protein identification against the Arabidopsis TAIR10

database (35,386 entries). Details on the parameters used are given in Supplementary Methods. The mass spectrometry proteomics data have been deposited to the ProteomeXchange Consortium via the PRIDE (Vizcaíno *et al.*, 2013; Deutsch *et al.*, 2017) partner repository with the dataset identifiers PXD012214 and PXD012215 (DRM/DSM distribution patterns) and PXD012248 (phosphoproteomics).

NO_3^- influx studies – Root NO_3^- influx was assayed as described (Laugier *et al.*, 2012). Details are given in Supplementary Methods.

Statistical analyses and data visualization – Functional classification of proteins was done based on Mapman (Thimm *et al.*, 2004) and Classification SuperViewer Tool (Provart & Zhu, 2003). Information about subcellular location was derived from SUBA3 (Tanz *et al.*, 2013). Detailed protein function was manually updated with the support of TAIR (Huala *et al.*, 2001). Other statistical analyses were carried out with Sigma Plot (version 11.0) and Excel (Microsoft, 2013). Heat maps were generated with R package *Superheat*. Over-representation analysis was done on PANTHER website via Fisher's exact test, p-values were adjusted using Bonferroni correction.

Results

Generation and characterization of a cbl1/4/5/8/9 mutant devoid of CBL Ca^{2+} sensors at the plasma membrane

In order to enable investigating the collective function of the CBL-CIPK network in decoding Ca^{2+} signals emanating at the PM we sought to create a mutant lacking all CBL-type Ca^{2+}-sensor proteins at this cellular compartment. To this end we pursued a crossing strategy involving previously published individual *cbl* mutants (Figure 1A). Initially, *cbl1-1* (Wassilewskija background) was crossed with *cbl9-1* (Columbia Col-0) resulting in a *cbl1-1/9-1* double mutant, which was five time back crossed with *cbl9-1* to create a double mutant in Col-0 background.

Subsequent crosses with *cbl5-2* and *cbl4* resulted in a quadruple *cbl* mutant (*cbl1*/*4*/*5*/*9* abbreviated as *cbl*4x) that combined loss-of-function alleles of all four CBL proteins, which are targeted to the PM by means of dual lipid modification through myristoylation and S-acylation (Supplementary Figure S1A). We subsequently pyramidized this quadruple mutant with *cbl8-1*, a mutant of a PM localized CBL protein, which is targeted to the PM by a myristoylation-independent mechanism (Batistic *et al.*, 2010). This created a quintuple mutant

(cbl1/4/5/8/9, abbreviated as *cbl*5x) in which the lack of PM localized CBL Ca^{2+} sensors prevents activation of downstream phosphorylation processes (Figure 1A).

Four independent homozygous *cbl5x* mutant lines (#3-2, #3-4, #3-5 and #4-1) were chosen for detailed molecular verification (Supplementary Figure S1B). All individual lines used to generate the cbl5x mutant were confirmed to carry loss-of-function alleles (Supplementary Figure S1B,C). Since it was previously observed that mutant pyramidization can result in up-regulation of related genes or compensatory effects causing residual transcripts in alleles harboring T-DNA insertions, we assayed the expression profile of all ten *CBL* genes causing in these lines as well as in the *cbl*4x line and in the *cbl1/9* double mutant obtained in our crossing scheme. We did not observe compensatory up-regulation of any non-mutated CBL gene in these lines (Figure 1B). However, we noted a reduction of detectable *CBL8* transcripts to around 50% of WT level in the *cbl4x* and *cbl1-1/9-1* mutant, suggesting that regulation of *CBL8* expression may be interconnected with proper expression of *CBL1* and *CBL9*. While we did not detect discernible transcript accumulation for *CBL4* and *CBL8* in the analyzed multiple mutant lines, residual transcripts for *CBL1, CBL5* and *CBL9* were detected. Notably, we did not detect such residual transcripts in the respective single mutants (Supplementary Figure 1C). In the case of *CBL5* and *CBL9* the positioning of the T-DNA insertion between the second and third and in the first EF hand, respectively, would prevent the translation of functional proteins from these transcripts. Since the T-DNA insertion in *cbl1-1* is located upstream of the initiation codon, and therefore the residual transcript of this gene could result in the formation of functional CBL1 protein, we quantitatively determined the accumulation of this transcript. Compared to WT, *CBL1* transcripts were strongly reduced, down to 7.4% in *cbl1/9*, to 8.3% in *cbl4x* and to 10% in *cbl5x.* Although statistical analyses did not support significance of the differences between these genotypes, they may suggest compensatory mechanisms as cause for transcript re-accumulation. A similar compensatory up-regulation was reported for a double mutant of the two closely related vacuolar Ca^{2+} sensors CBL2 and CBL3. Here, residual *CBL2* transcript was only detected in the *cbl2-1/cbl3* double mutant, but was absent in the *cbl2-1* single mutant prior to crossing (Eckert *et al.*, 2014).

To assess any potential impact of the impaired CBL-mediated decoding of PM born Ca^{2+} signals on the regular development we comparatively investigated the growth phenotypes of the multiple mutants. No matter if plants were grown in soil, hydroponically or on plates, we did not observe discernible differences in growth habitus or root growth between the different genotypes (Supplementary Figure 2). Moreover, we did not observe quantitative differences between WT and the respective mutants in fresh weight and root growth of plants when grown on 0.5x MS (Supplementary Figure 2).

Plasma membrane CBL-proteins exert multifaceted functions in regulating nitrate uptake and nitrate dependent modulation of primary and lateral root growth

Fluctuations in nitrate availability cause a complex array of root growth responses and adaptive adjustments of transport processes. We sought to study these multifaceted nutrient responses as a model case to enlighten the collective contribution of PM born Ca^{2+}-signaling via CBLs to these processes. To this end, we performed root growth assays in which seedlings were initially grown for 3 days on 0.5x MS agar plates and subsequently transferred for another 6 days to media with distinct nitrate concentrations ranging from 0 mM to 5 mM before the total root growth was scored.

Without external nitrate supply, no further primary root growth was observed for wild type (WT) and mutant, resulting in the same total primary root length of both genotypes after 6 days (Figure 2A,B). As previously reported, the gain of primary root length in WT progressively increased concomitant with increasing nitrate availability up to a concentration of 2 mM (Figure 2A,B). However, a further increase of media nitrate concentration to 5 mM did not cause further growth acceleration. In contrast, under low nitrate conditions (LN, 0.2 mM) the *cbl5x* mutant did not exhibit any gain of primary root growth when compared to conditions of absolute nitrate starvation suggesting that PM CBL function is essential for primary root growth under LN conditions that require activity of HATS. In contrast, under high nitrate conditions (HN, 5 mM) the *cbl5x*-mutant displayed longer roots than WT. The latter finding is indicative for a mis-regulated growth response of the mutant under conditions of LATS activity.

The *cbl5x* mutant also displayed a conditional phenotype in lateral root density. Significantly lower lateral root density was observed under nitrate starvation (0N), while with LN, the *cbl5x* mutant exhibited significantly higher lateral root density than WT (Figure 2C). This lateral root growth phenotype of the *cbl5x* mutant resembled that of mutants defective in the function of the nitrate transporter NRT2.1. Also *nrt2.1* shows a reduced repression of lateral root density upon increasing nitrate concentrations (Malamy & Ryan, 2001; Little *et al.*, 2005). Collectively, the range of phenotypes observed in the *cbl5x* mutant suggested nitrate concentration-dependent functions of CBLs in regulation of nitrate transport and signaling by affecting for example the membrane potential or directly the nitrate uptake transport.

In order to elucidate the potential contribution of collective CBL function to nitrate uptake under LN and HN conditions, we conducted nitrate influx assays under various nitrate regimes (Figure 2D,E). To this end, root nitrate uptake at external NO_3 concentration of 0.2 mM (LN) or 5 mM (HN) were determined in plants that

were either only nitrate starved for 5 days (-N), or resupplied with 1 mM nitrate for 1 or 4 hours. In general both, WT and *cbl5x* mutant plants exhibited higher nitrate influxes at HN compared to LN and in both conditions influx increased after transfer to 1 mM NO_3. When plants were starved for N, influx measurement at LN resulted in a significantly enhanced nitrate influx in *cbl5x* compared to WT. Such difference was not observed after transfer of the plants to nitrate prior to measurements. Conversely, nitrate influx measurements at HN conditions were only significantly lower in *cbl5x* than WT after transfer of the plants to 1 mM NO_3. These results reinforce the notion that the loss of PM CBL protein function triggers diverse deviations from WT regarding nitrogen related processes like root growth and nitrate uptake.

Loss of plasma membrane CBL function distinctively affects the phosphoproteome during nitrate responses and alters phosphorylation of nitrate transporters and proton pumps

CIPK-mediated phosphorylation of target proteins represents an almost immediate downstream effect of CBL-conferred Ca^{2+} signaling events. We therefore performed a comparative proteome profiling analysis of WT and *cbl5x* including conditions of nitrate starvation (0N) and conditions of LN and HN resupply (Figure 3). For this analysis, roots of hydroponically grown plants were subject to following experimental regimes: (i) nitrate starvation without nitrate resupply (0N), (ii) nitrate starvation with nitrate resupply of 0.2 mM nitrate for 5 min (low nitrate for short time, LNS), (iii) or for 15 min (low nitrate for longer time, LNL), (iv) nitrate starvation with nitrate resupply of 5 mM nitrate for 5 min (high nitrate for short time, HNS), (v) or for 15 min (high nitrate for longer time, HNL).

This approach allowed to quantify overall 1971 phosphopeptides representing 867 distinct proteins. K-means clustering was applied to this data set to systematically unravel characteristic patterns in the phosphorylation responses of WT and mutant in distinct conditions (Figure 4). The phosphopeptide responses grouped to 7 distinct clusters of peptides defined according to their mutant/WT phosphorylation level ratio (MWP) in the different conditions. One notable cohort of 14 peptides formed cluster 5 that represented peptides with generally lower MWP irrespective of the experimental conditions. These P-sites may represent targets of CBL mediated regulation that are not only under primary regulation by changes in nitrate supply. For 136 phosphopeptides, higher MWP was observed only at nitrate starvation, but no differences between genotypes were discernible at any time point upon LN or HN resupply (cluster 6). Notably, for cluster 7 comprising 33 phosphopeptides, a remarkable CBL-dependence in the specificity and speed of stimulus-induced changes of the phosphoproteome was revealed. Here, the original pattern at 0N changed within 5

minutes into distinct and specific patterns depending on the supplied nitrate (either LNS or HNS). This indicates that the absence of PM localized CBL function triggered distinct consequences in the immediate responses to low and high nitrate availability. However, the MWP ratio pattern further distinctly changed within 15 minutes depending on the nitrate availability (LNL and HNL). These MWPs suggest diverse contributions of CBL signaling to target protein phosphorylation during different phases of LN and HN supply. The k-means clustering approach was particularly informative with regard to the LNS conditions, suggesting a significant contribution of PM CBL function to this response. 90 phosphopeptides (cluster 1, and cluster 4) displayed a lower than WT phosphorylation level specifically in LNS conditions, while higher MWPs were observed in the other 4 experimental regimes. 160 proteins specifically displayed higher phosphorylation in the mutant compared to WT at LNS conditions (cluster 3 and cluster 7). Conversely, for 62 proteins (cluster 2) a significantly lower-than WT phosphorylation was observed in *cbl5x* specifically at LNS condition.

We subsequently inspected the data set to identify changes in MWP that may affect the activity or other functions of proteins related to nitrate responses and transport as well as proteins known to function in Ca^{2+} signaling or transport. Among the peptides that were less phosphorylated in *cbl5x* than WT in LNS condition (cluster 2) we noticed the C-terminal activation site of PM proton ATPases AHA1 and AHA2 at T948 and T947, the N-terminal phosphorylation site of NRT2.1 at S28, and the inhibitory phosphorylation sites of AMT1;1 at T460 and AMT1;2 at T472, while T464 of AMT1;3 was found in cluster 3. For the inhibitory phosphorylation sites of AMTs, a lower phosphorylation in *cbl5x* was observed at LNS and/or LNL (Supplementary Figure S3). Moreover, proteins with kinase activity and calcium ion binding proteins were over-represented in cluster 2. Among the only 14 proteins that were in general less phosphorylated in the *cbl5x* mutant (cluster 5) we noticed several aquaporins. Specifically, we observed reduced phosphorylation in *cbl5x* of C-terminal peptides of the aquaporins PIP2;1 (SLGSFRS(ph)AANV), PIP2;5 (ALGS(ph)FRS(ph)QPHV), PIP2;7 (ALGS(ph)FRS(ph)NATN), and PIP2;8 (ALAS(ph)FRS(ph)NPTN) (Supplementary Table S2, Supplementary Figure S3). A higher phosphorylation specifically at LNS in *cbl5x* was for example observed for N-terminal phosphopeptides of the Ca^{2+} ATPases ACA2 and ACA8, while ACA10 showed higher than wild type phosphorylation under HN (Supplementary Figure S3).

Our analysis also revealed a complex CBL-dependent phosphorylation pattern and modulation for the high affinity nitrate transporter NRT2.1 and PM ATPase AHA2 (Figure 5), while total protein abundance of these proteins did not change (Supplementary Figure S4). For NRT2.1 significantly distinct levels of phosphorylation between WT and *cbl5x* were detected for the inhibitory phosphorylation site S11 and the activating

phosphorylation site S28. Moreover, we discovered differential phosphorylation for the C-terminal phosphorylation site T521. Upon LN supply, an increase of S28 phosphorylation, which activates NRT2.1 (Li *et al.*, 2020) occurred in WT but was absent in *cbl5x* (Figure 5A). This lack of NRT2.1 activation corresponded with the reduced root growth of the mutant under these conditions. Interestingly, we detected an inverse modulation concerning the inhibitory P-site S11 in the mutant (Figure 5B) suggesting a coordinated regulation of NRT2.1 by the CBL-CIPK network under N starvation. The significantly lower phosphorylation levels of S11 in *cbl5x* under 0N conditions suggested higher activation of NRT2.1 and was concomitant with the observed higher nitrate influx during nitrate starvation in *cbl5x* (Figure 2D). In WT, LN and HN resupply for 15 minutes resulted in a decreased phosphorylation of NRT2.1 at C-terminal T521 (Figure 5C). Strikingly, in *cbl5x*, phosphorylation of T521 at LNS and HNL was significantly higher. No comparative quantitative information could be obtained for the NRT2.1 phosphorylation site S501 (Supplementary Table S2).

Furthermore, at LN the increase in phosphorylation of the C-terminal activation site of AHA2 at T947 was delayed and reduced in *cbl5x* compared to WT (Figure 5D). Such differences were not observed in response to HN supply. Moreover, also phosphorylation of the second activating P-site T881 was significantly lower in *cbl5x* than in WT under most conditions suggesting coordinated regulation of proton and nitrate fluxes (Figure 5E). Collectively, the observed changes in general phosphorylation pattern and the differences at specific P-sites support a coordinative role for the CBL-CIPK network in orchestrating the regulation of nitrate uptake and growth adaptation.

We also observed a noticeable correlation between the phosphorylation pattern of NRT2.1 and that of the CBL-regulated kinase CIPK25. In WT, phosphorylation of CIPK25 at T440 was positively correlated with phosphorylation of NRT2.1 at S11 and negatively correlated with NRT2.1 phosphorylation at S28 (Figure 5F). In *cbl5x*, phosphorylation of CIPK25 at T440 was significantly reduced at nitrogen starvation and at LN, but higher than WT at HN. These findings point to a co-regulation of NRT2.1 with CIPK25.

Loss of PM CBL function disturbs protein distribution between membrane phases

Protein phosphorylation not only regulates activities of PM proteins but also appears to affect the localization and distribution of these proteins in the PM subdomains (Prak *et al.*, 2008; Hao *et al.*, 2014). To ascertain the potential contribution of Ca^{2+} signaling via CBL proteins to these processes we sought to determine the nitrate-dependent modulation of protein distribution between detergent resistant (DRM) and detergent soluble (DSM) fractions within the PM in WT and *cbl5x* (Figure 3). Overall, we identified 4320 proteins in DRM

and DSM fractions in these analyses. Of these, 1734 proteins were identified in at least two biological replicates within a given treatment, and these were subsequently processed for comparative quantitation. Domain distribution of proteins within the PM was calculated as ratio of protein abundances in DRMs in relation to their abundance in DSMs. DRM/DSM ratios were then compared for nitrate resupplied condition and nitrate starvation conditions. Thereby, a relative increase in DRM/DSM ratio under nitrate resupply compared to nitrate starvation was considered indicative of an enrichment of proteins within membrane microdomains (DRM fraction) upon nitrate supply. A relative decrease of the DRM/DSM ratio under nitrate supply compared to nitrate starvation was considered indicative depletion of a protein from membrane microdomains.

We analyzed the distribution of CBLs and CIPKs in DRM and DSM fractions. Of the plasma membrane localized CBLs, CBL1 and CBL9 were the only members of the CBL-family identified in membrane microdomains fractions. CBL1 was significantly enriched in DRM fractions at HNL, while CBL9 was significantly depleted from DRM in LNS compared to nitrate starvation. This depletion from DRM was abrogated at LNL (Figure 6A). Considering that CBL9 represents an established regulator of NRT1.1, these findings suggest that differential domain association represents a facet of Ca^{2+} dependent regulation of nitrate transport processes.

Also for nitrate-related CIPKs we observed differential nitrate-dependent domain association. CIPK8 was depleted from DRM upon LN, but then significantly enriched in DRM fractions upon HN (Figure 6A). CIPK4 showed opposite DRM/DSM ratios to CIPK8. CIPK23 was identified to be depleted from DRM fractions under low and high nitrate supply compared to nitrate starvation (Figure 6A). The CBLs and CIPKs were not identified in the DRM/DSM fractions of *cbl5x*.

To comparatively illuminate the global modulation of DRM/DSM dynamics in WT and *cbl5x* in response to LN and HN, the DRM/DSM ratios of proteins quantified in both genotypes were classified by k-means clustering (Supplementary Figure S5). Proteins in clusters 1, 3, and 6 showed a generally lower than average abundance in DRM fractions (low DRM/DSM ratios). Thereby, cluster 3 contained proteins with very low DRM/DSM ratios, which were mainly co-purifying proteins, such as ribosomes (Zauber *et al.*, 2013). These proteins will therefore not be discussed further.

In contrast, proteins in clusters 2, 4 and 5 showed higher than average abundance in DRM fractions (high DM/DSM ratios), and these clusters were enriched by *bona fide* DRM proteins, such as remorins (Kierszniowska *et al.*, 2009). Cluster 4 contained proteins maintaining high DRM/DSM ratios under all

conditions in WT as well as in the *cbl5x* mutant. Among these, transporters such as ammonium transporters, aquaporins and ATPases were over-represented. Cluster 2 and cluster 5 contained proteins, for which in WT the DRM/DSM ratio increased under HNL, suggesting that these proteins were recruited to DRM upon short-term nitrate resupply. Interestingly, this DRM recruitment was absent in *cbl5x*. Instead, in *cbl5x* we observed an increased DRM/DSM ratio for cluster 2 and cluster 5 proteins at LNL. Thus, the recruitment to DRM for cluster 2 and 5 proteins was induced by HN in WT but by LN in *cbl5x* (Supplementary Figure S5). Direct comparison of DRM/DSM ratios in WT and *cbl5x* at all nitrate conditions (Supplementary Figure S6) revealed a pronounced enrichment of various proteins in DRM in *cbl5x* under LNL compared to WT. Interestingly, among these DRM-enriched proteins at LNL we identified six Ca^{2+}-dependent protein kinases (CPKs, CPK1, 7, 27, 28, 30, 32), four Ca^{2+}-ATPases (ACAs, ACA2, 8, 10, 11) and four aquaporins (PIPs, PIP1;3; PIP1;5, PIP2;1, PIP2;7) (Supplementary Figure S6, Supplementary Table S3).

The high fraction of proteins from the CPK signaling pathway (calcium ATPases and calcium-dependent protein kinases) among the proteins with significantly high enrichment in DRM under LNL is exemplified for CPK30 (Figure 6B), for which we also observed a stronger than WT enrichment in DRM of *cbl5x* mutant at HNS. These findings reveal that absence of effective CBL function at the PM impacts on the domain localization of Ca^{2+} signal decoding CPKs.

We also observed notable differences between genotypes in the DRM/DSM distribution of nitrate transporter NRT2.1 that correlated with genotype dependent root growth phenotypes and phosphorylation patterns. In WT, NRT2.1 significantly enriched in DRM at 15 minutes of nitrate resupply compared to nitrate starvation, irrespective of LN or HN concentration (Figure 6C). However, in *cbl5x* this enrichment of NRT2.1 in DRM was absent.

The nitrate availability also affected the domain distribution of proton ATPases. While AHA2 in WT was depleted from DRMs under LN, HNS triggered DRM enrichment (Figure 6D). Interestingly, loss of CBL function in *cbl5x* disturbed the DRM relocalization of AHA2 under HN conditions (Figure 6D). Together these data indicate not only that nitrate availability has profound influences on the membrane domain distribution of transporters and proton pumps, but also reveal that Ca^{2+}-dependent phosphorylation impacts on these processes.

Collectively, these data support the conclusion that Ca^{2+} signalling via Ca^{2+}-dependent protein phosphorylation exerts profound regulatory effects on PM protein composition during plant adaptation to

fluctuation in nitrate availability. Moreover, these data reveal that particularly nitrate transporters and proton pumps were subject to nitrate responsive PM domain translocation.

Discussion

Accumulating evidence points to multifaceted functions of the CBL-CIPK Ca^{2+} sensor protein kinase network in various physiological and adaptation processes in plants (Kudla *et al.*, 2018). However, an inherent feature of network-like signaling systems is their robustness to perturbation and ability to compensate the loss of individual components (Barabasi & Albert, 1999; Hetherington, 2001). This to some extent limits the study of such systems by reverse genetic analyses of individual mutants. To overcome such limitations we report and initially characterize a quintuple CBL mutant devoid of CBL-type Ca^{2+} sensors at the PM that allows to genetically approaching the contribution of this signaling network to PM borne signaling and regulatory processes. We aimed at deciphering the global role of the CBL-calcium-sensing system in PM signaling. It was not intended to specifically decipher the particular contribution of individual CBL proteins in these processes. Therefore analysis of the *cbl5x* mutant does not resolve to which extend a singular CBL contributes to the observed responses.

This *cbl5x* mutant may exhibit minor residual CBL1 activity; an aspect that needs to be considered, but very likely does not limit the suitability of this multiple mutant. Nevertheless, the apparent absence of discernible morphological phenotypes in this mutant appears surprising on first hand. Although this might suggest an exclusive function of PM CBL-CIPK signaling in adaptive responses but not in default developmental processes, we would consider such interpretation unlikely. Notably, double mutants of tonoplast localized CBLs exhibit dramatic developmental phenotypes (Eckert *et al.*, 2014). Moreover, Arabidopsis does not only harbor 26 Ca^{2+}-activated CIPKs, but also possesses 34 Ca^{2+}-regulated CDPKs (Cheng *et al.*, 2002; Luan, 2009). As most of the PM targeted CBLs, also the vast majority of these CDPKs appears to be subject to dual lipid-modification by myristoylation and S-acylation and therefore consequently may function in membrane domains shared with the CBL proteins (Saito *et al.*, 2018). This localization pattern would provide a mechanistic basis for compensatory CDPK function upon genetic perturbation of CBL function, which to some extent could suppress obviously discernible phenotypes. In line with such hypothesis we uncover an enhanced recruitment of several CDPKs into DRMs in various experimental conditions specifically in the *cbl5x* mutant. The potential

occurrence of such compensatory mechanisms should be considered in data interpretation of genetic approaches involving network perturbation.

The availability of the *cbl5x* mutant provides a unique resource for elucidating the contribution of the CBL-CIPK network to PM borne signaling processes and we used this tool to study its impact on nitrate related processes on several layers. Our phenotype analyses of primary and lateral root growth under LN and HN indicated multiple nitrate concentration dependent functions of PM CBL signaling in regulating these processes. PM CBL function appeared to be essential for conveying an appropriate response of primary root growth to limited nitrate supply indicating an essential role of these Ca^{2+} sensors in establishing high-affinity nitrate uptake. Moreover, also at HN primary root growth of *cbl5x* deviated from WT indicating a so far non-appreciated role of CBL-CIPK signaling in processes also under these conditions. These growth phenotypes concurred with significant alterations of nitrate influx in roots of *cbl5x* that again indicated distinct deviations from WT under LN and HN.

CBL proteins translate Ca^{2+} signals into downstream regulatory phosphorylation events by activating their interacting CIPKs. The profound and complex consequences of impaired PM CBL function on the root phosphoproteome at LN and HN identified here points to a prominent and multifaceted role of this signaling network in orchestrating nitrate responses in plants. Remarkably, especially under LN conditions, our results suggest a coordinative role of CBL-CIPK signaling. This becomes evident at level of individual proteins but also at level of co-regulating multiple proteins directly affecting nitrate transport (like different NRTs) and proteins indirectly modulating nitrate uptake (like AHAs and PIPs). So far, NRT1.1/NPF6.3 has been the only nitrate transporter known to be directly regulated by CBL-CIPK dependent phosphorylation (Ho *et al.*, 2009; Leran *et al.*, 2015). Here, we advance our mechanistic understanding of nitrate transport regulation by identifying NRT2.1 as subject of direct or indirect CBL- and thereby CIPK-mediated phospho-regulation. Although identity of the CIPK kinase exerting direct NRT2.1 phosphorylation remains to be determined, we consider a CIPK-independent role of CBLs for the observed differences in phosphorylation pattern rather unlikely. Remarkably, loss of CBL function inversely affected degree of phosphorylation of inhibitory and activating P-sites within NRT2.1 under N starvation, providing an example for coordinated regulation within an individual protein. In this way, reduced phosphorylation of the inhibitory residue S11 and enhanced phosphorylation of the activating residue S28 in LN conditions allows for effective activation of this high affinity nitrate transporter (Li *et al.*, 2020). Notably, also the nitrate transceptor NRT1.1 is subject to CBL-CIPK phosphorylation, which switches this transporter into the high affinity state (Ho *et al.*, 2009). Thereby, simultaneous regulation of

NRT1.1 and NRT2.1 (and most likely other NRTs) provides a mean for coordinated PM nitrate influx adjustment by the CBL-CIPK network.

Previously, mutational analyses of T460 in AMT1.1 revealed a negative regulatory role for phosphorylation of this residue and concomitantly CIPK23 has been identified as mediating this phosphorylation (Straub *et al.*, 2017). We provide *in vivo* evidence that indeed fluctuations in nitrate availability are causative for these changes in AMT phosphorylation level and that these changes depend on the function of CBL Ca^{2+} sensors. These findings and the above described nitrate modulated PM CBL-CIPK-dependent phosphorylation of AHAs and PIPs further extends the concept of concerted multicomponent regulation of plant nitrate acquisition.

The specific results of our phosphoproteome analysis allow to postulate the following model of coordinated regulation of nitrate responses (Figure 7): (i) LN exposure leads to in NRT2.1 activation by phosphorylation at activating S28, and by dephosphorylation at inhibitory S11 (Li *et al.*, 2020) in a CBL-dependent manner to facilitate HATS. Accordingly, in *cbl5x* we detected significantly lower S11 phosphorylation, especially after nitrogen starvation and at LN resupply for 15 minutes. These differences are in line with the observed higher nitrate uptake rates of nitrate starved *cbl5x* plants. (ii) LN induced CBL-dependent phosphorylation of the PM proton pump AHA2 at activating T947 and T881 contributing to enhanced cellular H+ extrusion to support/enable/facilitate $H+/NO_3^-$-co-transport by NRT2.1. (iii) Simultaneously, in LN conditions CBL-dependent phosphorylation of AMT1.1 and AMT1.3 at T460 and T464 reduces the uptake capability of roots for NH_4^+ in favor of promoting optimized nitrate uptake and metabolic consumption. Complementary to this optimization of HATS conveyed nitrate uptake in LN, aquaporins were detected with lower phosphorylation levels but with higher persistence in DRM in *cbl5x* indicating that also water influx rates are coordinately regulated by CBL function and thereby in turn can affect solute uptake as well as cell elongation and growth. Collectively, these regulatory events confer coordinated adaptation of plants to limited nitrate availability and an efficient function of uptake systems under these conditions.

Moreover, we discovered a positive correlation between phosphorylation of CIPK25 in its C-terminal regulatory domain at T440 and phosphorylation of NRT2.1 at S11. CIPK25 function has been linked to regulation of root growth, and C-terminal phosphorylation of other CIPKs has been reported to modulate their activity (Guo *et al.*, 2002; Yang *et al.*, 2019; Tagliani *et al.*, 2020). Therefore, coordinated activity regulation of CIPK25 and NRT2.1 might be meaningful for implementing nitrate responses. It would either allow for a CIPK25-mediated regulation of NRT2.1 or alternatively, but not mutually exclusive, would enable

that CIPK25 phosphorylates further substrates to convey regulating root growth in coordination with regulation of NRT2.1 activity.

Such a concomitant co-regulation of nitrate transport related proteins raises the question how such a mechanism may become spatially and mechanistically implemented. To address this point we sought to gain insights into the general membrane domain dynamics during nitrate responses and domain distribution of nitrate related proteins by determining the DRM and DSM composition at various nitrate supply regimes. Our results support the conclusion that loss of CBL function at the PM significantly affects the domain distribution of many proteins and impairs translocation of several proteins into DRMs. Previous reports have highlighted the importance of protein phosphorylation for regulating their lateral mobility and membrane domain distribution with NADPH oxidases and aquaporins serving as prime examples (Prak *et al.*, 2008; Han *et al.*, 2019). However, it remained unknown if and how Ca^{2+} signaling would be linked to these phosphorylation mediated regulatory processes. Our finding that loss of PM CBL Ca^{2+} sensor function simultaneously affects protein phosphorylation of NRT2.1, AHAs and PIPs as well as their domain distribution, provides first evidence that at least during responses to fluctuating nitrate availability Ca^{2+} signaling, protein phosphorylation and protein domain distribution may be functionally interconnected. This newly emerging exciting facet of plant signaling deserves further detailed elucidation.

Acknowledgments

We thank Adrian Hills (Laboratory of Plant Physiology and Biophysics, University of Glasgow) for us detailed user guides for EZ-R_{HIZO} software. We thank Anette Mähs for analyzing *CBL* transcript levels and Katrin Held and Stefanie Schültke for help in generating genetic material used in this study. The work was supported by an international grant from the ANR in France (SIPHON ANR-13-ISV6-0002-01) and Deutsche Forschungsgemeinschaft (SCHU1533/8-1) in Germany.

Author contribution

LCC: performed proteomics experiments and data analysis DRM, participated in writing of the paper. JNO: performed the crossings leading to *cbl5x*, and initial phenotypic characterization of *cbl5x*; LS: writing of the paper, data analysis; XNW: data analysis proteomics; LX: nitrate phenotype analysis, ZL: phosphoproteomics

data analysis workflow, AJ: nitrate uptake experiments, LL: nitrate uptake experiments, JK: design of the study, writing of the paper, WXS: design of the study, data analysis, writing of the paper.

References

Armengaud P, Zambaux K, Hills A, Pattison RJ, Blatt MR, Amtmann A. 2009. EZ-Rhizo: integrated software for the fast and accurate measurement of root system architecture. *Plant Journal* **57**(5): 945-956.

Barabasi AL, Albert R. 1999. Emergence of scaling in random networks. *Science* **286**(5439): 509-512.

Batistic O, Rehers M, Akerman A, Schlucking K, Steinhorst L, Yalovsky S, Kudla J. 2012. S-acylation-dependent association of the calcium sensor CBL2 with the vacuolar membrane is essential for proper abscisic acid responses. *Cell Res* **22**(7): 1155-1168.

Batistic O, Sorek N, Schultke S, Yalovsky S, Kudla J. 2008. Dual fatty acyl modification determines the localization and plasma membrane targeting of CBL/CIPK Ca^{2+} signaling complexes in *Arabidopsis*. *Plant Cell* **20**(5): 1346-1362.

Batistic O, Waadt R, Steinhorst L, Held K, Kudla J. 2010. CBL-mediated targeting of CIPKs facilitates the decoding of calcium signals emanating from distinct cellular stores. *Plant J* **61**(2): 211-222.

Bhat RA, Panstruga R. 2005. Lipid rafts in plants. *Planta* **223**(1): 5-19.

Camanes G, Bellmunt E, Garcia-Andrade J, Garcia-Agustin P, Cerezo M. 2012. Reciprocal regulation between AtNRT2.1 and AtAMT1.1 expression and the kinetics of NH_4^+ and NO_3^- influxes. *J Plant Physiol* **169**(3): 268-274.

Cheng SH, Willmann MR, Chen HC, Sheen J. 2002. Calcium signaling through protein kinases. The Arabidopsis calcium-dependent protein kinase gene family. *Plant Physiology* **129**: 469-485.

Cox J, Mann M. 2008. MaxQuant enables high peptide identification rates, individualized p.p.b.-range mass accuracies and proteome-wide protein quantification. *Nature Biotechnology* **26**(12): 1367-1372.

Crawford NM. 1995. Nitrate: Nutrient and signal for plant growth. *The Plant Cell* **7**: 859-868.

Demir F, Hontrich C, Blachutzik JO, Scherzer S, Reinders Y, Kierszniowska S, Schulze WX, Harms GS, Hedrich R, Geiger D, et al. 2013. *Arabidopsis* nanodomain-delimited ABA signaling pathway regulates the anion channel SLAH3. *Proceedings of the National Academy of Sciences of the USA* **110**(20): 8296-8301.

Deutsch EW, Csordas A, Sun Z, Jarnuczak A, Perez-Riverol Y, Ternent T, Campbell DS, Bernal-Llinares M, Okuda S, Kawano S, et al. 2017. The ProteomeXchange consortium in 2017: supporting the cultural change in proteomics public data deposition. *Nucleic Acids Res* **45**(D1): D1100-D1106.

Eckert C, Offenborn JN, Heinz T, Armarego-Marriott T, Schultke S, Zhang C, Hillmer S, Heilmann M, Schumacher K, Bock R, et al. 2014. The vacuolar calcium sensors CBL2 and CBL3 affect seed size and embryonic development in *Arabidopsis thaliana*. *Plant J* **78**(1): 146-156.

Engelsberger WR, Schulze WX. 2012. Nitrate and ammonium lead to distinct global dynamic phosphorylation patterns when resupplied to nitrogen starved Arabidopsis seedlings. *The Plant Journal* **69**(6): 978-995.

Fuglsang AT, Kristensen A, Cuin T, Schulze WX, Persson J, Thuesen KH, Ytting CK, Oehlschlaeger C, Mahmood K, Sondergaard TE, et al. 2014. Receptor kinase mediated control of primary active proton pumping at the plasma membrane. *The Plant Journal* **80**(6): 951-964.

Gazzarrini S, Lejay L, Gojon A, Nonnemann O, Frommer WB, von Wirén N. 1999. Three functional transporters for constitutive, diurnally regulated, and starvation-induced uptake of ammonium into *Arabidopsis* roots. *The Plant Cell* **11**: 937-947.

Guo Y, Xiong L, Song CP, Gong D, Halfter U, Zhu JK. 2002. A calcium sensor and its interacting protein kinase are global regulators of abscisic acid signaling in Arabidopsis. *Developmental Cell* **3**: 233-244.

Han JP, Koster P, Drerup MM, Scholz M, Li S, Edel KH, Hashimoto K, Kuchitsu K, Hippler M, Kudla J. 2019. Fine-tuning of RBOHF activity is achieved by differential phosphorylation and Ca^{2+} binding. *New Phytol* **221**(4): 1935-1949.

Hao H, Fan L, Chen T, Li R, Li X, He Q, Botella MA, Lin J. 2014. Clathrin and Membrane Microdomains Cooperatively Regulate RbohD Dynamics and Activity in Arabidopsis. *Plant Cell* **26**(4): 1729-1745.

Haruta M, Sabat G, Stecker K, Minkoff BB, Sussman MR. 2014. A peptide hormone and its receptor protein kinase regulates plant cell expansion. *Science* **343**: 408-411.

Hermans C, Hammond JP, White PJ, Verbruggen N. 2006. How do plants respond to nutrient shortage by biomass allocation? *Trends in Plant Science* **11**(12): 610-617.

Hetherington AM. 2001. Guard cell signaling. *Cell* **107**(6): 711-714.

Ho C-H, Lin SH, Hu HC, Tsay YF. 2009. CHL1 functions as a nitrate sensor in plants. *Cell* **138**(6): 1184-1194.

Hu HC, Wang YY, Tsay YF. 2009. AtCIPK8, a CBL-interacting protein kinase, regulates the low-affinity phase of the primary nitrate response. *Plant Journal* **57**(2): 264-278.

Huala E, Dickerman AW, Garcia-Hernandez M, Weems D, Reiser L, LaFond F, Hanley D, Kiphart D, Zhuang M, Huang W, et al. 2001. The Arabidopsis Information Resource (TAIR): a comprehensive database and web-based information retrieval, analysis, and visualization system for a model plant. *Nucleic Acids Research* **29**(1): 102-105.

Kierszniowska S, Seiwert B, Schulze WX. 2009. Definition of Arabidopsis sterol-rich membrane microdomains by differential treatment with methyl-ß-cyclodextrin and quantitative proteomics. *Molecular and Cellular Proteomics* **8**(4): 612-623.

Kolukisaoglu U, Weinl S, Blazevic D, Batistic O, Kudla J. 2004. Calcium sensors and their interacting protein kinases: genomics of the Arabidopsis and rice CBL-CIPK signaling networks. *Plant Physiol* **134**(1): 43-58.

Krapp A, David LC, Chardin C, Girin T, Marmagne A, Leprince AS, Chaillou S, Ferrario-Mery S, Meyer C, Daniel-Vedele F. 2014. Nitrate transport and signalling in Arabidopsis. *J Exp Bot* **65**(3): 789-798.

Krouk G, Crawford NM, Coruzzi GM, Tsay YF. 2010. Nitrate signaling: adaptation to fluctuating environments. *Current Opinion in Plant Biology* **13**: 266-273.

Kudla J, Becker D, Grill E, Hedrich R, Hippler M, Kummer U, Parniske M, Romeis T, Schumacher K. 2018. Advances and current challenges in calcium signaling. *New Phytol* **218**(2): 414-431.

Laugier E, Bouguyon E, Mauriès A, Tillard P, Gojon A, Lejay L. 2012. Regulation of high-affinity nitrate uptake in roots of Arabidopsis depends predominantly on posttranscriptional control of the NRT2.1/NAR2.1 transport system. *Plant Physiology* **158**(2): 1067-1078.

Leran S, Edel KH, Pervent M, Hashimoto K, Corratge-Faillie C, Offenborn JN, Tillard P, Gojon A, Kudla J, Lacombe B. 2015. Nitrate sensing and uptake in Arabidopsis are enhanced by ABI2, a phosphatase inactivated by the stress hormone abscisic acid. *Sci Signal* **8**(375): ra43.

Leran S, Varala K, Boyer JC, Chiurazzi M, Crawford N, Daniel-Vedele F, David L, Dickstein R, Fernandez E, Forde B, et al. 2014. A unified nomenclature of NITRATE TRANSPORTER 1/PEPTIDE TRANSPORTER family members in plants. *Trends in Plant Science* **19**(1): 5-9.

Li Z, Wu XN, Jacquot A, Lejay L, Schulze WX. 2020. A phospho-switch in the N-terminus of NRT2.1 affects nitrate uptake by controlling the interaction of NRT2.1 with NAR2.1. *bioRxiv* **2020/898254**. doi: https://doi.org/10.1101/2020.01.08.898254

Little DY, Rao H, Oliva S, Daniel-Vedele F, Krapp A, Malamy JE. 2005. The putative high-affinity nitrate transporter NRT2.1 represses lateral root initiation in response to nutritional cues. *Proc Natl Acad Sci U S A* **102**(38): 13693-13698.

Liu KH, Diener A, Lin Z, Liu C, Sheen J. 2020. Primary nitrate responses via calcium signalling and diverse protein phosphorylation. *J Exp Bot*. **71**(15): 4428-4441

Liu KH, Niu Y, Konishi M, Wu Y, Du H, Sun Chung H, Li L, Boudsocq M, McCormack M, Maekawa S, et al. 2017. Discovery of nitrate-CPK-NLP signalling in central nutrient-growth networks. *Nature* **545**(7654): 311-316.

Luan S. 2009. The CBL–CIPK network in plant calcium signaling. *Trends in Plant Science* **14**(1): 39-42.

Malamy JE, Ryan KS. 2001. Environmental regulation of lateral root initiation in Arabidopsis. *Plant Physiol* **127**(3): 899-909.

Malinsky J, Operkarova M, Grossman G, Tanner W. 2013. Membrane microdomains, rafts, and detergent-resistant membranes in plants and fungi. *Annual Review of Plant Biology* **64**: 501-529.

Martiniere A, Fiche JB, Smokvarska M, Mari S, Alcon C, Dumont X, Hematy K, Jaillais Y, Nollmann M, Maurel C. 2019. Osmotic Stress Activates Two Reactive Oxygen Species Pathways with Distinct Effects on Protein Nanodomains and Diffusion. *Plant Physiol* **179**(4): 1581-1593.

Menz J, Li Z, Schulze W, Ludewig U. 2016. Early nitrogen-deprivation responses in Arabidopsis roots reveal distinct differences on transcriptome and (phospho-)proteome levels between nitrate and ammonium nutrition. *The Plant Journal*. **88**(5): 717-734

Mlodzinska E, Klobus G, Christensen MD, Fuglsang AT. 2015. The plasma membrane H^+ -ATPase AHA2 contributes to the root architecture in response to different nitrogen supply. *Physiol Plant* **154**(2): 270-282.

Pertl H, Himly M, Gehwolf R, Kriechbaumer R, Strasser D, Michalke W, Richter K, Ferreira F, Obermeyer G. 2001. Molecular and physiological characterisation of a 14-3-3 protein from lily pollen grains regulating the activity of the plasma membrane H^+ ATPase during pollen grain germination and tube growth. *Planta* **213**(1): 132-141.

Prak S, Hem S, Boudet J, Viennois G, Sommerer N, Rossignol M, Maurel C, Santoni V. 2008. Multiple phosphorylations in the C-terminal tail of plant plasma membrane aquaporins: role in subcellular trafficking of AtPIP2;1 in response to salt stress. *Molecular and Cellular Proteomics* **7**(6): 1019-1030.

Provart N, Zhu T. 2003. A browser-based functional classification SuperViewer for *Arabidopsis* genomics. *Currents in Computational Molecular Biology*: 271-273.

Remans T, Narcy P, Pervent M, Girin T, Tillard P, Lepetit M, Gojon A. 2006. A central role for the nitrate transporter NRT2.1 in the integrated morphological and physiological responses of the root system to nitrogen limitations in *Arabidopsis*. *Plant Physiology* **140**: 909-921.

Riveras E, Alvarez JM, Vidal EA, Oses C, Vega A, Gutierrez RA. 2015. The Calcium Ion Is a Second Messenger in the Nitrate Signaling Pathway of *Arabidopsis*. *Plant Physiol* **169**(2): 1397-1404.

Rocks O, Peyker A, Kahms M, Verveer PJ, Koerner C, Lumbierres M, Kuhlmann J, Waldmann H, Wittinghofer A, Bastiaens PI. 2005. An acylation cycle regulates localization and activity of palmitoylated Ras isoforms. *Science* **307**(5716): 1746-1752.

Saito S, Hamamoto S, Moriya K, Matsuura A, Sato Y, Muto J, Noguchi H, Yamauchi S, Tozawa Y, Ueda M, et al. 2018. N-myristoylation and S-acylation are common modifications of Ca^{2+}-regulated *Arabidopsis* kinases and are required for activation of the SLAC1 anion channel. *New Phytol* **218**(4): 1504-1521.

Sanchez-Barrena MJ, Chaves-Sanjuan A, Raddatz N, Mendoza I, Cortes A, Gago F, Gonzalez-Rubio JM, Benavente JL, Quintero FJ, Pardo JM, et al. 2020. Recognition and activation of the plant AKT1 potassium channel by the kinase CIPK23. *Plant Physiol*. **182**(4): 2143-2153

Scheible WR, Morcuende R, Czechowski T, Fritz C, Osuna D, Palacios-Rojas N, Schindelasch D, Thimm O, Udvardi MK, Stitt M. 2004. Genome-wide reprogramming of primary and secondary metabolism, protein synthesis, cellular growth processes, and the regulatory infrastructure of *Arabidopsis* in response to nitrogen. *Plant Physiology* **136**(1): 2483-2499.

Schlesier B, Breton F, Mock HP. 2003. A hydroponic culture system for growing *Arabidopsis thaliana* plantlets under sterile conditions. *Plant Molecular Biology Reporter* **21**: 449-456.

Sorek N, Poraty L, Sternberg H, Bar E, Lewinsohn E, Yalovsky S. 2007. Activation status-coupled transient S acylation determines membrane partitioning of a plant Rho-related GTPase. *Mol Cell Biol* **27**(6): 2144-2154.

Straub T, Ludewig U, Neuhauser B. 2017. The Kinase CIPK23 Inhibits Ammonium Transport in Arabidopsis thaliana. *Plant Cell* **29**(2): 409-422.

Szymanski W, Kierszniowska S, Schulze WX. 2013. Metabolic labeling and membrane fractionation for comparative proteomic analysis of *Arabidopsis thaliana* suspension cell cultures. *Journal of Visualized Experiments* **79**: e50535.

Tagliani A, Tran AN, Novi G, Di Mambro R, Pesenti M, Sacchi GA, Perata P, Pucciariello C. 2020. The calcineurin beta-like interacting protein kinase CIPK25 regulates potassium homeostasis under low oxygen in Arabidopsis. *J Exp Bot*. **71**(9): 2678-2689

Tang R-J, Liu H, Yang L, Gao X-S, Garcia VJ, Luan S, Zhang H-X. 2012. Tonoplast calcium sensors CBL2 and CBL3 control plant growth and ion homeostasis through regulating V-ATPase activity in *Arabidopsis*. *Cell Research* **22**: 1650-1665.

Tanz SK, Castleden I, Hooper CM, Vacher M, Small I, Millar HA. 2013. SUBA3: a database for integrating experimentation and prediction to define the SUBcellular location of proteins in Arabidopsis. *Nucleic Acids Research* **41**: D1185-1191.

Thimm O, Bläsing O, Gibon Y, Nagel A, Meyer S, Kruger P, Selbig J, Muller LA, Rhee SY, Stitt M. 2004. MAPMAN: a user-driven tool to display genomics data sets onto diagrams of metabolic pathways and other biological processes. *The Plant Journal* **37**(6): 914-939.

Vidal EA, Alvarez JM, Araus V, Riveras E, Brooks M, Krouk G, Ruffel S, Lejay L, Crawford N, Coruzzi GM, et al. 2020. Nitrate 2020: Thirty years from transport to signaling networks. *Plant Cell*. **32**(7): 2094-2119

Vizcaíno JA, Côté RG, Csordas A, Dianes JA, Fabregat A, Foster JM, Griss J, Alpi E, Birim M, Contell J, et al. 2013. The PRoteomics IDEntifications (PRIDE) database and associated tools: status in 2013. *Nucleic Acids Research* **41**(1): D1063-D1069.

Wang YY, Hsu PK, Tsay YF. 2012. Uptake, allocation and signaling of nitrate. *Trends in Plant Science* **17**(8): 458-467.

Weinl S, Kudla J. 2009. The CBL-CIPK Ca^{2+}-decoding signaling network: function and perspectives. *New Phytologist* **2009**(184): 3.

Wisniewski JR, Zougman A, Nagaraj N, Mann M. 2009. Universal sample preparation method for proteome analysis. *Nature Methods* **6**(5): 359-362.

Wu X, Sanchez-Rodriguez C, Pertl-Obermeyer H, Obermeyer G, Schulze WX. 2013. Sucrose-induced receptor kinase SIRK1 regulates a plasma membrane aquaporin in *Arabidopsis*. *Molecular and Cellular Proteomics* **12**(10): 2856-2873.

Wu XN, Chu L, Xi L, Pertl-Obermeyer H, Li Z, Sklodowski K, Sanchez-Rodriguez C, Obermeyer G, Schulze WX. 2019. Sucrose-induced Receptor Kinase 1 is Modulated by an Interacting Kinase with Short Extracellular Domain. *Mol Cell Proteomics* **18**(8): 1556-1571.

Wu XN, Xi L, Pertl-Obermeyer H, Li Z, Chu LC, Schulze WX. 2017. Highly Efficient Single-Step Enrichment of Low Abundance Phosphopeptides from Plant Membrane Preparations. *Frontiers in Plant Science* **8**: 1673.

Xu J, Li H-D, Chen L-Q, Wang Y, Liu L-L, He L, Wu W-H. 2006. A protein kinase, interacting with two calcineurin B-like proteins, regulates K^+ transporter AKT1. *Cell* **125**: 1347-1360.

Yang Y, Wu Y, Ma L, Yang Z, Dong Q, Li Q, Ni X, Kudla J, Song C, Guo Y. 2019. The Ca^{2+} Sensor SCaBP3/CBL7 Modulates Plasma Membrane H^+-ATPase Activity and Promotes Alkali Tolerance in Arabidopsis. *Plant Cell* **31**(6): 1367-1384.

Zauber H, Szymanski WG, Schulze WX. 2013. Unraveling sterol-dependent membrane phenotypes by analysis of protein abundance-ratio distributions in different membrane fractions under biochemical and endogenous sterol-depletion. *Molecular and Cellular Proteomics* **12**(12): 3732-3743.

Supporting Information

Figure S1: Information about individual *cbl*-mutants.

Figure S2: Comparative developmental characterization of WT and mutant lines.

Figure S3: Phosphorylation of selected phosphopeptides of AMTs, ACAs and PIPs.

Figure S4: Normalized protein abundance of NRT2.1 and AHA2.

Figure S5: k-mean clustering of DRM/DSM abundance ratios of proteins identified in WT and *cbl5x* under 0.2 mM nitrate (LN) and 5 mM nitrate (HN) resupply.

Figure S6: Nitrate-dependent modulation of protein distribution in plasma membrane domains.

Methods S1 - Supplementary Methods

Supplementary Table S1: List of used primer for genotyping and quantitative real time PCR (qRT-PCR).

Supplementary Table S2: Data sheet **pPeptide_summary.**

Supplementary Table S3: Protein distribution ratios between DRM and DSM as log2(DRM/DSM) values for WT and *cbl5x*.

Figures

Figure 1: Generation of the *Arabidopsis thaliana cbl5x* mutant. (**A**) Crossing scheme for generation of the *cbl1/9* double (*cbl1-1/cbl9-1*), the *cbl* quadruple (*cbl4x*, *cbl1-1/cbl4/cbl5-2/cbl9-1*) and quintuple mutant (*cbl5x*, *cbl1-1/cbl4/cbl5-2/cbl8-1/cbl9-1*). Female and male crossing partners are indicated. Ws, Wassilewskija ecotype; Col-0, Columbia ecotype. (**B**) qRT PCR transcript analyses of *CBL* genes in Col-0, *cbl1/9*, *cbl4x* and *cbl5x*. *ACT2* served as internal reference. Means ± SE of three biological replicates. *cbl4x* (*cbl1-1/cbl4/cbl5-2/cbl9-1*); *cbl5x* (*cbl1-1/cbl4/cbl5-2/cbl8-1/cbl9-1*); *cbl1/9* (*cbl1-1/cbl9-1*).

Figure 2: Root growth phenotypes and ^{15}N-influx analyses of wild type and *cbl5x*. (**A**) Representative *Arabidopsis* plants at day 6 of growth of vertical agar plates without nitrate (0N), with 0.2 mM nitrate (LN) and 5 mM nitrate (HN). Scale bar: 1 cm. (**B**) Primary root length after 6 days of cultivation on the indicated media. (**C**) Lateral root density after 6 days of cultivation on the indicated media. (**D,E**) Nitrate influx analyses determined by $K^{15}NO_3$-influx upon exposure to 0.2 mM (**D**) or 5 mM (**E**) nitrate after pre-treatment. For pre-treatment, seedlings were initially grown at 1mM NH_4NO_3, exposed to nitrate starvation for 5 days and subsequently either kept in nitrate starvation (-N) or supplied with 1mM KNO_3 for 1 hour or 4 hours. In (B) and (C) mean with standard deviation of at least 50 seedlings is displayed. Asterisks indicate significant differences of *cbl5x* mutant to wild type: *** $p < 0.001$, * $p < 0.05$ by pairwise comparisons using Oneway ANOVA Holm-Sidak method.

Figure 3: Schematic depiction illustrating the experimental design of the comparative proteomic experiments. **0N**: nitrate starvation (-N for 2 days). **LNS**: resupply of 0.2 mM nitrate for 5 min. **LNL**: resupply of 0.2 mM nitrate for 15 min. **HNS**: resupply of 5 mM nitrate for 5 min. **HNL**: resupply of 5 mM nitrate for 15 min. *Arabidopsis thaliana* was used as a model organism.

Figure 4: Cluster analysis of peptides displaying differential phosphorylation. k-mean clustering of log_2-fold changes of phospho-peptide LFQ-values in *Arabidopsis cbl5x* compared to wild type (WT) was performed on peptides prepared from samples obtained after nitrate starvation (0N), resupply of 0.2 mM nitrate (LNS, LNL) and resupply of 5 mM nitrate (HNS, HNL). Color code represents log_2-fold change of *cbl5x* vs WT (blue: down-regulated in *cbl5x*; red: up-regulated in *cbl5x*).

Figure 5: Phosphorylation dynamics of selected peptides in NRT2.1 and AHA2. *Arabidopsis* NRT2.1 phosphorylation at (**A**) serine S28. (**B**) serine S11. (**C**) threonine T521. Phosphorylation of AHA2 at (**D**) threonine T947 and (**E**) threonine T881. (**F**) Phosphorylation of CIPK25 at threonine T440. In all panels, averages with standard deviations of three biological replicates are displayed. Small letters indicate significant differences in wild type (WT) relative to nitrate starvation conditions upon 0.2mM nitrate supply. Capital letters indicate significant differences in WT relative to nitrate starvation at 5mM nitrate supply. Asterisks indicate significant differences in *cbl5x* compared to wild type: *** p <0.001, ** p<0.01, * p<0.05 by pairwise comparisons using Oneway ANOVA Holm-Sidak method. ND: not detected.

Figure 6: DRM/DSM distribution of Ca^{2+} signaling components and nitrate related proteins from *Arabidopsis thaliana*. DRM/DSM distribution of (**A**) CBL and CIPK proteins detected in these analyses, (**B**) calcium-dependent protein kinase CPK30, (**C**) nitrate transporter NRT2.1, and (**D**) plasma membrane proton ATPase AHA2 detected in these analyses. DRM/DSM distribution ratios were calculated as nitrate supplied condition relative to nitrate starvation condition. In all panels, averages with standard deviations of three biological replicates are displayed. Small letters indicate significant differences in WT at 0.2 mM nitrate supply relative to nitrate starvation conditions, capital letters indicate significant differences in WT at 5mM nitrate supply relative to nitrate starvation. Asterisks indicate significant differences of *cbl5x* to WT within a given condition with at least p<0.05 by pairwise comparisons using Oneway ANOVA Holm-Sidak method.

Figure 7: Model of the *Arabidopsis* CIPK/CBL network in coordinated regulation of membrane transporters. At nitrate starvation (0N) NRT1.1 is activated as high affinity transporter (Ho *et al.*, 2009), while NRT2.1 is inactivated by phosphorylation at S11. LN supply results in activation of NRT2.1 by phosphorylation of S28 and de-phosphorylation at S11. Plasma membrane ATPases are activated at T947 and T881. AMTs are inactivated by phosphorylation at T460/T464. NRT1.1 is shown without borders to indicate its phosphorylation was not measured here, but has been well established in literature (Ho *et al.*, 2009).

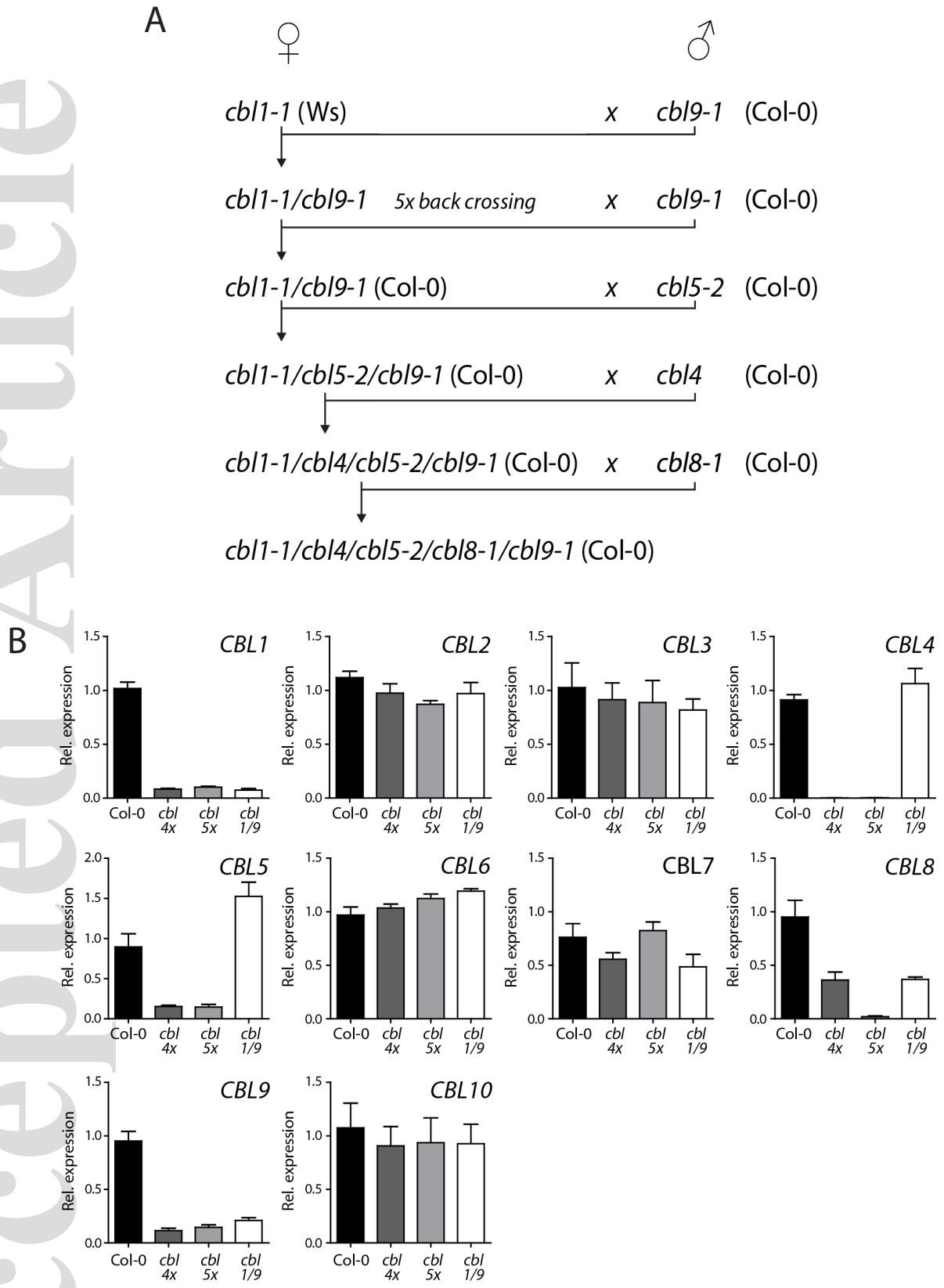

Figure 1

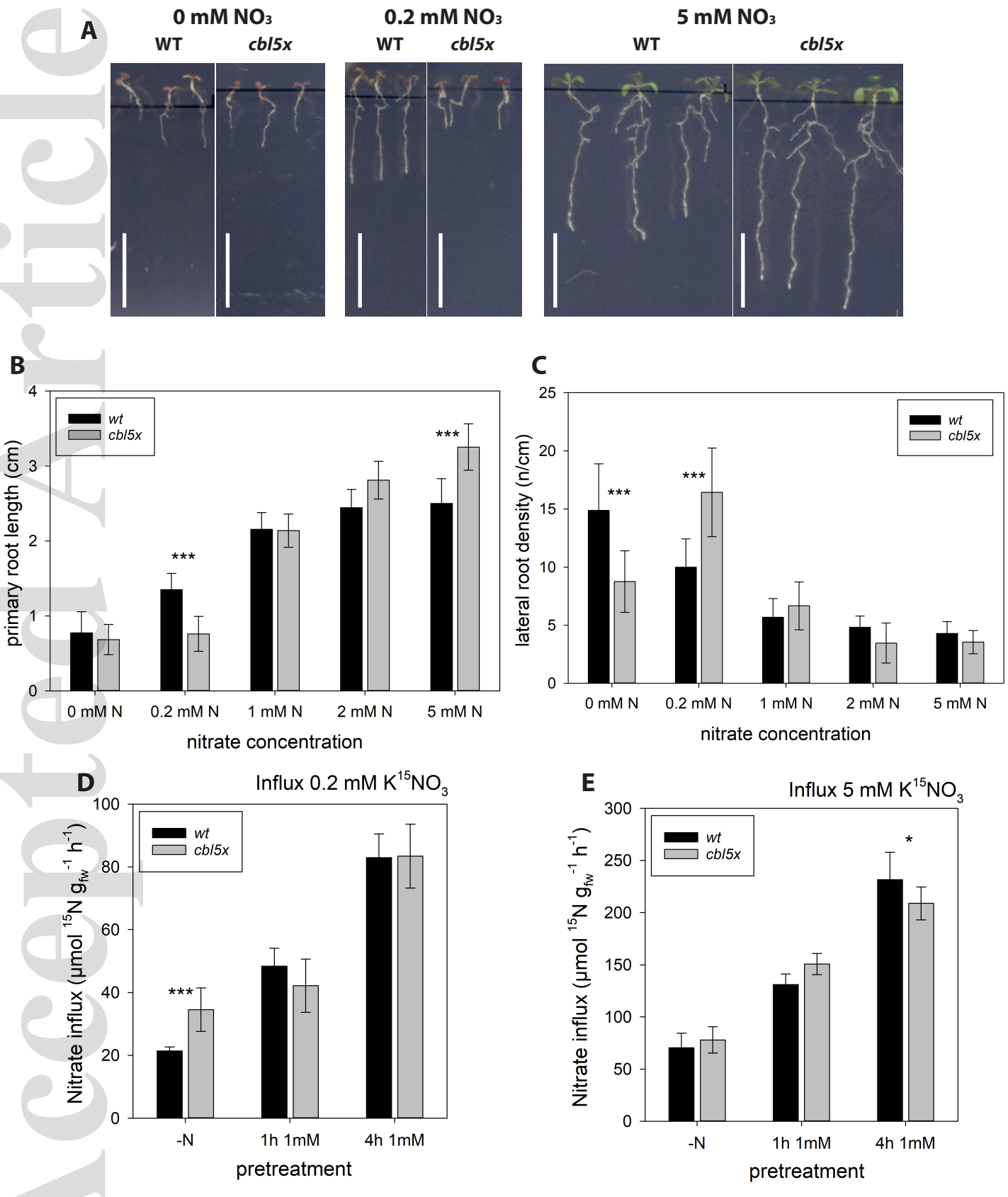

Figure 2

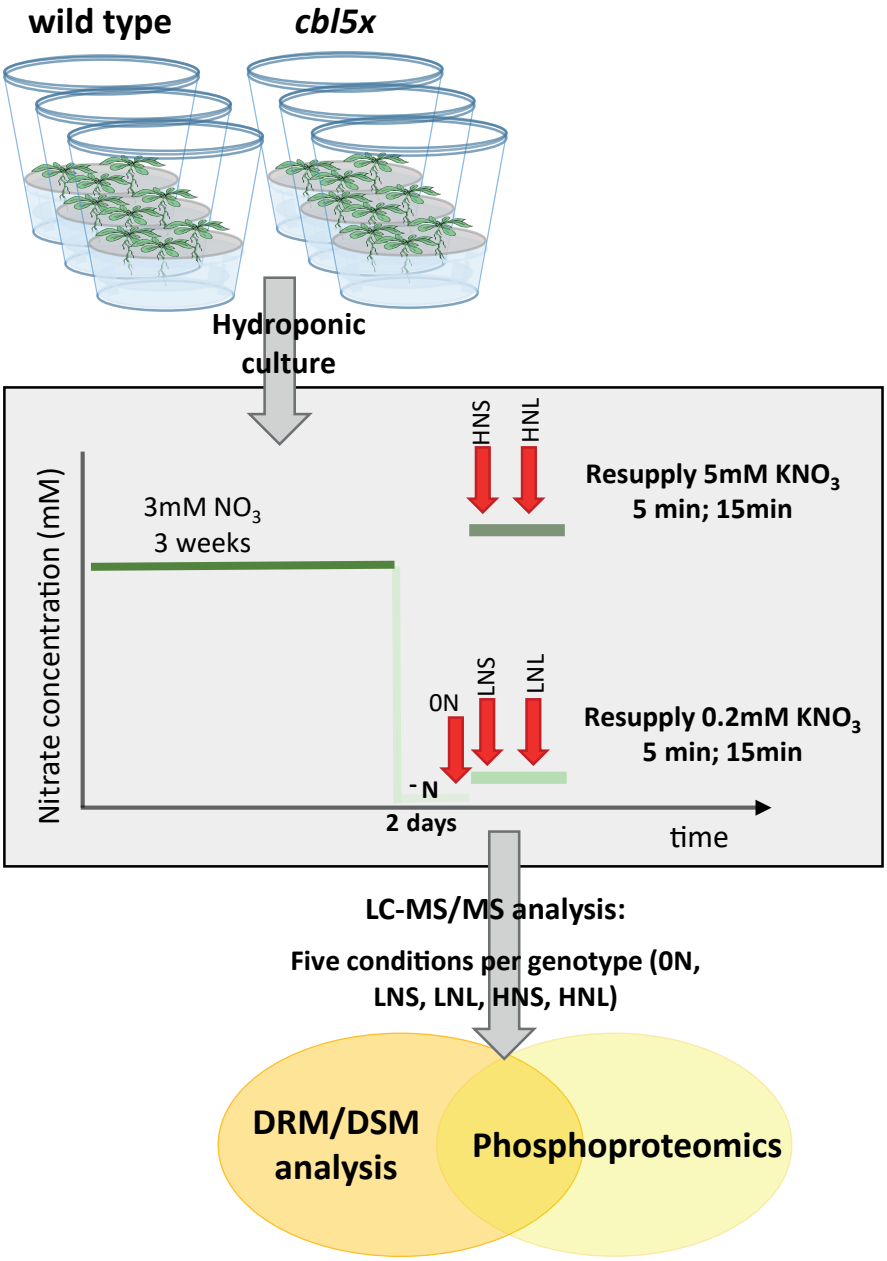

Figure 4